Kinetic and Calorimetric Evidence for Two Distinct Scaffolding Protein Binding Populations within the Bacteriophage P22 Procapsid†

Matthew H. Parker,‡,§,|| Christie G. Brouillette,*,‡ and Peter E. Prevelige, Jr.*,§

Laboratory for Biological Calorimetry, Biomolecular Analysis Group, Center for Biophysical Science and Engineering, and Department of Microbiology, University of Alabama at Birmingham, Birmingham, Alabama 35294

Received November 14, 2000; Revised Manuscript Received May 15, 2001

ABSTRACT: A wide variety of viruses require the transient presence of scaffolding proteins to direct capsid assembly. In the case of bacteriophage P22, a model in which the scaffolding protein selectively stabilizes on-pathway growing intermediates has been proposed. The stoichiometry and thermodynamics of binding of the bacteriophage P22 scaffolding protein within the procapsid were analyzed by light scattering and isothermal titration calorimetry. Calorimetric experiments carried out between 10 and 37 °C were consistent with the presence of at least two distinct populations of binding sites, in agreement with kinetic evidence obtained by a light scattering assay. Binding to the high-affinity sites occurred at 20 °C with a stoichiometry of approximately 60 scaffolding molecules per procapsid and an apparent K_d of approximately 100−300 nM and was almost completely enthalpy-driven. For the second binding population, precise fitting of the data was impossible due to small heats of binding, but the thermodynamics of binding were clearly distinct from the high-affinity phase. The heat capacity change (ΔC_p) of binding was large for the high-affinity sites and negative for both sets of sites. Addition of sodium chloride (1 M) greatly reduced the magnitude of the apparent ΔH, in agreement with previous evidence that electrostatic interactions play a major role in binding. A mutant scaffolding protein that forms covalent dimers (R74C/L177I) bound only to the high-affinity sites. These data comprise the first quantitative measurements of the energetics of the coat protein/scaffolding protein interaction.

The *Salmonella typhimurium* bacteriophage P22 provides a useful model system for the assembly of double-stranded DNA (dsDNA)[1] phage (*1, 2*) and viruses, including pathogenic members of the herpesvirus (*3*−*8*) and adenovirus (*9*) groups. An understanding of viral assembly pathways may lead to new approaches to the development of antiviral drugs (*10*). Furthermore, knowledge of the mechanisms of viral self-assembly may provide insights for the development of other self-assembling systems such as molecular machines.

The first step in the assembly of P22 is the polymerization of 420 molecules of the coat protein into a spheroid shell (the "procapsid") with $T = 7$ icosahedral symmetry (*11*−*13*). Because P22 expresses only a single coat protein gene product, the geometry of the structure mandates that this protein adopt a different, quasi-equivalent, conformation or set of binding interactions at each of the seven symmetry-related positions within the procapsid (*13*−*15*). The coat protein cannot accomplish this efficiently without the assistance of a scaffolding protein, which serves as an "assembly chaperone" and ensures that the coat proteins are added to the growing structure in the proper orientations. The scaffolding protein leaves the procapsid during DNA packaging, probably via holes that have been observed in the procapsid lattice (*12*), after which the procapsid expands by approximately 10% in radius, closes the holes, and becomes competent for attachment of the final proteins involved in assembly of an infectious phage (*16*).

The P22 scaffolding protein is a 303-residue, highly flexible and elongated molecule which appears to consist of several helical sections separated by turns and random coil regions (*17*). Analytical ultracentrifugation has revealed that the scaffolding protein forms a mixture of monomers, dimers, and tetramers at physiologically relevant and experimentally accessible concentrations. A mutant scaffolding protein (R74C/L177I) containing a single cysteine residue forms covalent dimers and assembles procapsids more rapidly in vitro than the wild-type protein, suggesting that scaffolding protein dimerization is important for assembly (*18*). The role of the tetrameric form is not known, but several lines of evidence suggest that both dimers and tetramers of the scaffolding protein participate in assembly (*13, 15, 19, 20*).

Scaffolding and coat proteins can be purified, and when mixed together in vitro assemble particles that closely resemble procapsids. When the wild-type scaffolding protein

† This work was supported by National Institutes of Health Grant GM47980 (to P.E.P.). M.H.P. was supported by NIH Postdoctoral Training Grant T32-AI07150.

* To whom correspondence should be addressed. C.G.B.: Phone (205) 975-5469, Fax (205) 934-0480, E-mail christie@cmc.uab.edu. P.E.P.: Phone (205) 975-5327, Fax (205) 975-5479, E-mail prevelig@uab.edu.

‡ Laboratory for Biological Calorimetry.

§ Department of Microbiology.

|| Current address: Vertex Pharmaceuticals, Inc., 130 Waverly St., Cambridge, MA 02139.

[1] Abbreviations: dsDNA, double-stranded DNA; GuHCl, guanidine hydrochloride; bis-ANS, 1,1′-bis(4-anilinonaphthalene-5-sulfonic acid); ITC, isothermal titration calorimetry; HEPES, *N*-(2-hydroxyethyl)-piperazine-*N*′-2-ethanesulfonic acid; PIPES, piperazine-*N*,*N*′-bis(2-ethanesulfonic acid).

10.1021/bi0026167 CCC: $20.00
Published on Web 06/27/2001

is supplied in molar excess, approximately 250−300 molecules are found within each procapsid (*21*), the same number as are found in vivo (*22, 23*). However, when the scaffolding to coat protein ratio is reduced to levels where scaffolding protein concentration is limiting, procapsids are assembled that contain as few as 50−150 scaffolding molecules (*21*). Parallel experiments using an assembly competent deletion mutant consisting of residues 141−303 demonstrated that a similar limiting number of molecules is sufficient for assembly with the truncated scaffolding protein. However, at least twice as many molecules (>600) of the 141−303 scaffolding protein fragment can bind within the procapsid when it is supplied in molar excess (*24*).

These results suggest that there are at least two distinct sets of binding sites for the scaffolding protein. One subset is required for assembly, but the other may simply serve to stabilize the structure and/or to prevent host proteins from becoming trapped inside the procapsid (*25*). The former population appears to have a well-defined number of binding sites that does not depend on the size of the scaffolding protein, while the latter population appears to be influenced by steric factors.

We have used isothermal titration calorimetry (ITC) to analyze the binding of the scaffolding protein to procapsid "shells" from which the scaffolding protein had been extracted. ITC can give a complete thermodynamic profile of a binding reaction, including values for binding affinity, ΔH, $\Delta S°$, and ΔC_p. Processes with multiple sets of binding sites can also be analyzed, and the stoichiometries of binding for each population can be determined. The results of these equilibrium experiments were compared to those obtained by analysis of the kinetics of binding by light scattering measurements.

MATERIALS AND METHODS

Preparation of Proteins. P22 procapsids were obtained as described previously (*21*). Briefly, phage containing amber mutations in DNA packaging genes were used to infect *Salmonella typhimurium* cells. After lysis of the bacteria, procapsids were harvested by centrifugation and purified by size-exclusion chromatography. Empty procapsid "shells" were obtained by repeated extraction with 0.5 M GuHCl followed by sedimentation through a solution of 10% (w/w) sucrose in buffer B (50 mM Tris-HCl, 25 mM NaCl, 2 mM EDTA, pH 7.6). SDS−PAGE indicated that the shells were >98% pure coat protein. Shells were dialyzed into buffer B and stored at 4 °C.

The GuHCl extracts were used to isolate the wild-type scaffolding protein by ion-exchange chromatography (*18, 21*). The R74C/L177I mutant scaffolding protein was purified from procapsids using a slightly different procedure (*18*). For most of the calorimetric experiments, the scaffolding protein was expressed in *E. coli* using a plasmid containing the genes for the coat, scaffolding, and portal proteins (L. Sampson and S. Casjens, unpublished results), and purified using the same method as for the R74C/L177I mutant. Scaffolding protein deletion mutants consisting of residues 141−303 and 141−292 were expressed from plasmids in *E. coli* and purified as described previously (*26, 27*). SDS−PAGE indicated that all scaffolding proteins were >99% pure, and the R74C/L177I covalent dimeric mutant contained <1% of the reduced monomeric protein. All scaffolding proteins were stored at −20 °C in buffer B or the corresponding HEPES or PIPES buffer. Calorimetric experiments were performed in these buffers; light scattering experiments were carried out in buffer B.

Scaffolding Protein Re-entry Kinetics. Scaffolding proteins were added to a solution of shells (0.40 mg/mL final concentration; 20 nM assuming 420 coat protein subunits per procapsid) in a cuvette maintained at 20 °C. Re-entry and binding were monitored by following the increase in the apparent absorbance at 250 nm due to light scattering. For Figure 1, wild-type or R74C/L177I scaffolding protein was added to give a final concentration of 670 scaffolding protein subunits per procapsid (expressed in terms of the monomer); wild-type was also added to a final concentration of 120 subunits per procapsid. Data were collected at 6 s intervals for the first 35 min (0.5 s read-average time), followed by a further 220 min at 45 s intervals (2 s read-average time). For Figure 2, R74C/L117I was added to the shells at a final concentration of 490 subunits per procapsid. After 20 min, an additional 490 subunits per procapsid of R74C/L177I, wild-type, or the assembly active deletion mutant consisting of residues 141−303, or an aliquot of buffer, were added. Data were collected at 7.5 s intervals (1 s read-average time) over 150 min. Initial A_{250} values were corrected for dilution and the addition of scaffolding protein as described previously (*28*).

Isothermal Titration Calorimetry. Solutions of procapsid shells at 0.88 mg/mL (45 nM) were placed into the 1.39 mL sample cell of a VP-ITC titration calorimeter (MicroCal, Inc., Northampton, MA). Scaffolding proteins were placed into a 250 μL injection syringe (the actual usable volume of which is about 290 μL) at 4.0 mg/mL (120 μM). After a delay of 60 s, a single injection of 1.5 μL was made (the data from which were discarded), followed at 300 s intervals by 34 injections of 8.5 μL each. For experiments conducted with the R74C/L177I scaffolding mutant, the concentrations of shells and scaffolding protein were 0.60 and 2.7 mg/mL, respectively. For the experiments conducted in 1 M NaCl, the scaffolding protein concentration in the syringe was increased to 5.6 mg/mL in order to allow complete saturation to be reached; 47 injections of 6.1 μL each were made. The cell contents were stirred at 250 rpm, and the cell temperature was maintained at 20 (±0.02) °C unless otherwise indicated. For each experiment, blank runs were also performed in which buffer was substituted for the procapsid shells. Data were analyzed by the method of Wiseman et al. (*29*) using version 5.0 of Origin (MicroCal, Inc.). The normalized ΔH plots for each of the blank titrations were smoothed by fitting to a second-order exponential decay function, and the smoothed blank data sets were then subtracted from the scaffolding protein/shell data sets.[2,3] The corrected data were fit to a model incorporating two independent sets of binding sites to obtain the apparent binding stoichiometries, ΔH values, and association constants for each of the binding populations. Heat capacity changes were determined by performing experiments at 10, 20, 30, and 37 °C and calculating the dependence of ΔH values on temperature, assuming that ΔC_p is constant within the temperature range of the experiments.

RESULTS

The Kinetics of Scaffolding Protein Binding to Procapsid Shells Suggest That at Least Two Binding Populations Exist. When procapsids are treated with low concentrations of guanidine hydrochloride (GuHCl), the scaffolding and other minor proteins are extracted, leaving "shells" consisting solely of coat protein. Based on electron cryomicroscopic image analysis, removal of the scaffolding protein results in, at most, minimal changes in the coat protein lattice (*15*). When purified scaffolding protein is added back to these shells, it re-enters and binds, a process that can be followed by light scattering. Greene and King (*30*) observed that, when the scaffolding protein was supplied in molar excess (560 scaffolding subunits per procapsid), the re-entry process could be approximated by 2 exponentials with relaxation times of approximately 1 and 45 min. However, when the scaffolding protein concentration was lowered to where it corresponded to 140 subunits per procapsid, the slower phase essentially disappeared. Extraction of the scaffolding protein from procapsids by treatment with bis-ANS also displayed two kinetic phases (*31*).

Figure 1 illustrates this point. Scaffolding protein re-entry and binding were followed by recording the increase in the apparent absorbance at 250 nm due to light scattering for the following: wild-type scaffolding protein supplied in molar excess (670 scaffolding subunits per procapsid), a limiting amount of wild-type scaffolding protein (120 subunits per procapsid), and a covalently cross-linked dimeric mutant scaffolding protein, R74C/L177I (*18*), supplied in molar excess (335 covalent dimers per procapsid). The slower phase was nearly absent for the wild-type scaffolding protein when its concentration was limiting. This phase was also absent for the covalent dimeric mutant, even when it was supplied in excess. However, when wild type was supplied in excess, two distinct kinetic phases were observed, and the amplitude of the light scattering change at the end of the experiment was higher than for either of the other two experiments. This suggests that the faster phase reflects the binding of scaffolding protein dimers, while the slower phase primarily involves the binding of additional monomers.

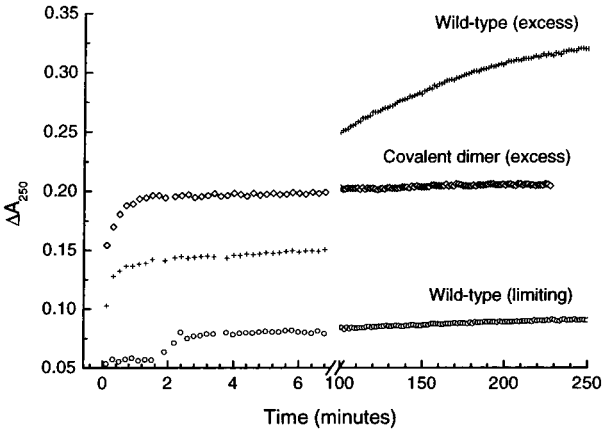

FIGURE 1: Kinetics of scaffolding protein binding to empty procapsid "shells" suggest that multiple binding populations exist and that scaffolding protein dimers can bind to only one set of sites. A solution of procapsid shells was placed into a cuvette maintained at 20 °C in a spectrophotometer. Solutions of the wild-type scaffolding protein or the R74C/L177I covalent dimeric mutant were added, and the increase in light scattering due to binding was monitored by following the apparent absorbance at 250 nm. The dead time for mixing was 5−10 s. Procapsids have a normal complement of 250−300 scaffolding molecules per shell. The wild-type scaffolding protein was supplied either in molar excess (670 molecules per procapsid) or in a substoichiometric amount (120 molecules). The covalent dimeric mutant was supplied in molar excess (335 dimers per procapsid).

The Covalent Dimeric Mutant Scaffolding Protein Does Not Participate in the Second Phase of Binding. The data presented in Figure 1, along with previously obtained results (*24*, *28*, *30*), suggest that the wild-type scaffolding protein binds to procapsid shells with at least two kinetic phases. This suggests that at least two distinct populations of bound scaffolding protein exist within the procapsid. The R74C/L177I covalent dimeric mutant, however, did not display the slower kinetic phase. This suggests that all of the scaffolding proteins are capable of binding rapidly to one subset of binding sites, but that the covalent dimeric mutant cannot bind to the second subset.

To test this, the R74C/L177I mutant was added to a solution of procapsid shells and allowed to equilibrate for 20 min, at which point the increase in light scattering had ceased. A second aliquot of either the wild-type scaffolding protein, a truncated scaffolding protein consisting of residues 141−303 (*24*, *27*), the R74C/L177I covalent dimeric mutant, or buffer was then added. The light scattering data were corrected for dilution and for the increase in absorbance caused by the second additions of scaffolding protein and are presented in Figure 2. The addition of the second aliquot

[2] This smoothing step was necessary due to the low signal-to-noise ratio in the data. We tested several exponential and polynomial fitting routines and found that a second-order exponential decay consistently gave the most random distribution of residuals (see also footnote 3). Attempts were also made to eliminate the large heat signal of the dissociation of scaffolding protein oligomers by performing "inverse titrations": shells were placed in the syringe, and small volumes were injected into a solution of scaffolding protein in the cell. However, dilution of the shells also had a large heat signal that changed exponentially as the titration proceeded (data not shown). Moreover, to cover an appropriate range of scaffolding/shell ratios, very high concentrations of shells and low concentrations of scaffolding protein were required, resulting in very low signal-to-noise ratios.

[3] The blank titrations of scaffolding protein into buffer displayed a significant heat signal, due in part to the dissociation of scaffolding protein oligomers upon dilution into the cell (Figure 3A). The intensity of these signals decreased as the degree of dilution decreased in subsequent injections. Methods have been developed for determining the thermodynamic parameters for dissociation of dimeric proteins by ITC (*52*, *55*). However, this could not be successfully applied for the P22 scaffolding protein due to its complex self-association behavior into dimers and tetramers (*18*) and the inability to completely populate the oligomeric forms at accessible protein concentrations. Based on the dissociation constants for dimers and tetramers determined by analytical ultracentrifugation (*18*), the weight percentage of dimers reaches a maximum of 32% at approximately 4 mg/mL scaffolding protein at 20 °C, and then decreases as tetramers begin to predominate. Even at 50 mg/mL, the weight percentage of tetramers is only about 80%. Graverson et al. (*53*) encountered similar difficulties when studying dimeric plasminogen kringle domains by ITC, in that they were unable to fit the dissociations due to strong statistical correlations. We have addressed this problem by using two different methods of correcting for scaffolding protein dilution: a second-order exponential smoothing of the blank titrations (see Materials and Methods) and a linear regression of the final 5−10 points of the blank titrations. Values obtained using both blank-correction methods are listed in Tables 1 and 2. Like Graverson (*53*), we have used K_d' and $\Delta G^{\circ\prime}$ to denote that these are *apparent* association constants which may be influenced by scaffolding protein oligomer dissociation. In Figures 3−5, data corrected by the exponential smoothing method are shown; curves of very similar shape were obtained in all cases using the other blank-correction method.

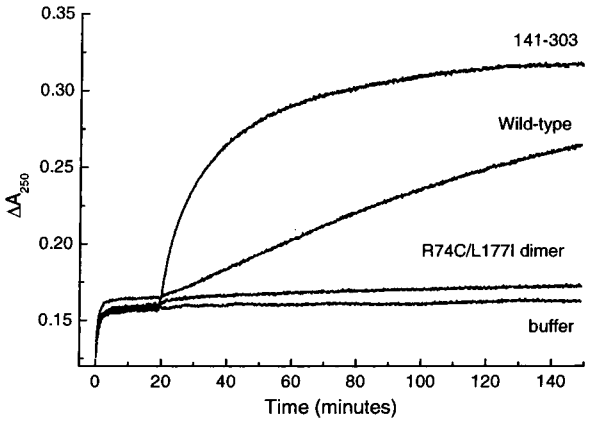

FIGURE 2: Covalent dimeric scaffolding protein mutant does not bind to the set of sites that have slower binding kinetics. The covalent dimeric R74C/L177I mutant (490 molecules per procapsid, expressed in terms of monomeric subunits) was added to a solution of procapsid shells at 20 °C. After 20 min, an additional 490 subunits per procapsid of R74C/L177I, wild-type, or an assembly active truncated scaffolding protein consisting of residues 141−303 were added. For a negative control, buffer was added instead. The apparent absorbance at 250 nm due to light scattering was used to follow binding. The A_{250} values after the addition of the second aliquots were adjusted for dilution and for the additional absorbance of each scaffolding protein that was added.

of R74C/L177I resulted in very little increase in light scattering compared to the addition of buffer. However, addition of either the wild-type or the 141−303 scaffolding protein resulted in marked increases in light scattering. When the order of addition was reversed (i.e., wild-type scaffolding protein was allowed to bind for 20 min, followed by the addition of a second aliquot of wild-type, R74C/L177I, or buffer), the added wild-type protein caused a higher rate of increase in light scattering compared to the addition of buffer, while R74C/L177I did not (data not shown). These results suggest that the wild-type scaffolding protein or the 141−303 deletion mutant can bind to the second population of sites after the rapidly bound sites are occupied, but the covalent dimeric mutant cannot.

While these findings provide strong evidence for the existence of at least two separate binding populations, the amount of light scattering observed is probably not directly proportional to the number of scaffolding protein molecules bound within the procapsid. We therefore used ITC to obtain more quantitative information about the thermodynamics and stoichiometry of binding.

Isothermal Titration Calorimetry Confirms the Existence of Two Binding Populations. ITC can be used to determine the binding affinity, enthalpy change (ΔH), and stoichiometry of a binding interaction. The entropy change ($\Delta S°$) and heat capacity change (ΔC_p) can then be obtained from this information. If multiple binding populations exist, this can often be detected by ITC, and the stoichiometries of binding for each population can be determined.

The binding of scaffolding protein to coat protein monomers cannot be analyzed directly due to the additional heat signals accompanying the formation of coat−coat protein interactions that occur as the procapsid is assembled. Therefore, we investigated the binding of scaffolding protein to procapsid shells, as this gives insight into the scaffolding/coat interactions that occur within the procapsid. The scaffolding protein was injected into a stirred solution of

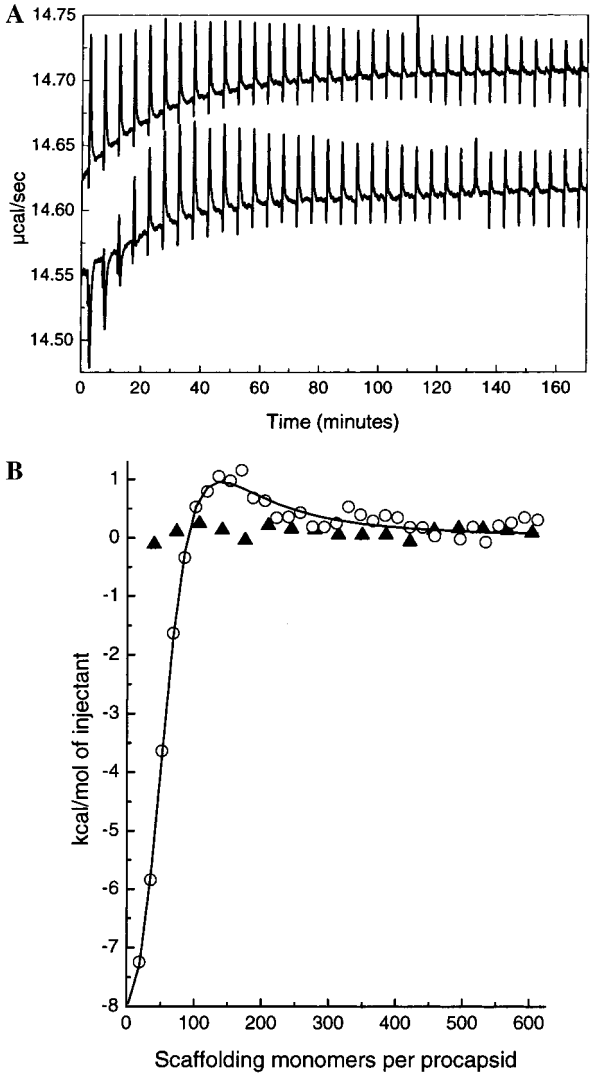

FIGURE 3: Binding of the scaffolding protein within the procapsid occurs with two distinct thermodynamic phases. ITC experiments were carried out in three different buffers at 20 °C, pH 7.6, as described in the text; the experiment performed in Tris buffer is shown. (A) Raw data for the titration of scaffolding protein into procapsid shells (lower trace) and scaffolding protein into buffer (upper trace). (B) Integrated heats for each injection were normalized, blank-corrected as described in the text, and plotted against the molar ratio of scaffolding protein subunits to procapsid shells for the scaffolding protein (open circles) and an inactive deletion mutant consisting of residues 141−292 (filled triangles). Data for the full-length scaffolding protein were fit to a model that incorporates two sets of binding sites (*29*).

procapsid shells at 20 °C in either PIPES, HEPES, or Tris buffer at pH 7.6. For each set of conditions, blank titrations were also performed, in which the scaffolding protein was injected into buffer in order to correct for heats of dilution and of scaffolding protein oligomer dissociation.[3] In each of these buffers, two distinct thermodynamic phases were observed (Figure 3).[4] Data were fit to a model that incorporates two separate sets of binding sites. The averages of the fitted parameters for experiments carried out in the three buffers are listed in Table 1. The high-affinity popula-

[4] As a negative control, an assembly inactive truncated scaffolding protein consisting of residues 141−292 (*24, 27*), which is missing part of the carboxyl-terminal coat protein binding domain, was also analyzed by ITC (Figure 3B). No binding was observed.

Table 1: Thermodynamic Parameters for the High-Affinity Binding Sites of the P22 Scaffolding Protein[a]

stoichiometry[b]	61 (7); 61 (10)
K_d' (nM)	300 (180); 91 (12)
$\Delta G^{\circ\prime}$ (kcal mol^{-1})	−8.7 (0.3); −9.4 (0.1)
$\Delta H'$ (kcal mol^{-1})	−11 (2); −6.5 (0.2)
$\Delta S^{\circ\prime}$ (cal mol^{-1} K^{-1})	−7.2 (6.9); +10 (1)
$\Delta C_p'$ (cal mol^{-1} K^{-1})[c]	−680 (45); −530 (80)

[a] For each parameter, the value obtained by using an exponentially smoothed blank correction (see text) is listed first, followed by the value obtained by instead correcting with a linear regression of the final 5−10 points of the blank titration.[3] Values in parentheses are standard deviations returned by the curve-fitting program and propagated as described by Casella and Berger (*54*). Values for all parameters except for $\Delta C_p'$ were obtained at 20 °C; $\Delta C_p'$ values were obtained from data collected at 10, 20, 30, and 37 °C. Stoichiometry, K_d', $\Delta G^{\circ\prime}$, $\Delta H'$, $\Delta S^{\circ\prime}$, and $\Delta C_p'$ values were the average of experiments carried out in three different buffers as described in the text. All values are *apparent* values as explained in footnote 3. All experiments were conducted at pH 7.6. [b] Number of scaffolding protein monomers bound per procapsid, assuming 420 coat protein subunits per procapsid. [c] Determined from the slopes of the lines in Figure 4E.

tion had a stoichiometry at 20 °C of approximately 60 scaffolding molecules per procapsid. The low-affinity population had much smaller heats of binding, rendering a precise fit of these data impossible**.** The high-affinity population had a negative $\Delta H'$ value at 20 °C. Despite the small heat signals for the low-affinity phase, it is clear that this population had a positive $\Delta H'$ value at 20 °C and that binding was driven by the favorable $\Delta S^{\circ\prime}$ term.

To determine whether protons are transferred between the buffer and the scaffolding/coat complex during binding, the apparent ΔH values were obtained in three buffers that have different enthalpies of ionization (*32*, *33*). No *systematic* variation of apparent ΔH with buffer ionization enthalpy was observed (data not shown), although considerable variation in apparent ΔH was observed for the high-affinity population when the exponential-smoothing method for blank correction was used (Table 1).

The Heat Capacity Changes for Both Binding Populations Are Negative. ITC experiments were carried out at 10, 20, 30, and 37 °C in HEPES buffer in order to measure the variation of $\Delta H'$ with temperature for each binding population. This gives the heat capacity change upon binding at constant pressure (ΔC_p), a parameter that provides information about the degree of solvent expulsion that accompanies binding (*34*−*36*). For the high-affinity binding sites, $\Delta H'$ became more negative as the temperature was raised (Figure 4, Tables 1and 2), indicating that $\Delta C_p'$ is negative. While a $\Delta C_p'$ value could not be calculated for the low-affinity binding sites, comparison of Figure 4A through Figure 4D shows that $\Delta H'$ clearly becomes more negative as the temperature is increased, and thus $\Delta C_p'$ is negative.

Electrostatic Interactions Contribute to Binding. The coat protein binding domain of the scaffolding protein consists of about 30 residues at the extreme carboxyl terminus (*24*, *27*). The NMR structure of this domain indicates that it contains two short amphipathic α-helices, connected by a five-residue loop, that bind to each other through hydrophobic interactions (*37*). A group of positively charged amino acids on one face of this domain appears to be involved in binding to the coat protein, as 1 M NaCl completely inhibits procapsid assembly in vitro and partially inhibits binding of the scaffolding protein to procapsid shells (*28*). (No further increase in inhibition is observed above 1 M NaCl.)

To analyze the effects of high ionic strength on the thermodynamics of scaffolding/coat protein binding, ITC experiments were conducted at 20 °C in HEPES buffer containing 1 M NaCl. The presence of 1 M NaCl reduced the magnitude of the exothermic heat signal by close to 10-fold (data not shown). These data could not be analyzed accurately due to the very small heat signals. Attempts to increase the magnitude of the signal were hampered by the large quantities of scaffolding protein that would be required (for example, 40−50 mg per experiment for a 10-fold increase in signal). The effects of ionic strength on the binding thermodynamics will be examined in detail at a later time. Nevertheless, it is clear that high ionic strength dramatically affects the thermodynamics of scaffolding/coat binding, as has been suggested previously (*28*).

Scaffolding Protein Dimers Bind Only to the High-Affinity Sites. The data shown in Figures 1 and 2 suggest that the covalently cross-linked dimeric scaffolding mutant R74C/L177I can bind to only one set of sites. To examine this, we performed ITC experiments at 20 °C in HEPES buffer using R74C/L177I. As shown in Figure 5, the dimeric form of the scaffolding protein bound to only one set of sites, with a stoichiometry of approximately 35 covalent dimers per procapsid. The data could not be fit to a model that incorporates two sets of binding sites. This suggests that the scaffolding protein binds to the high-affinity binding sites as a dimer and to the low-affinity sites primarily as a monomer.

DISCUSSION

Inhibition of viral assembly, or misdirection of assembly into nonviable structures, could provide a novel approach for antiviral drug design (*10*). Understanding the molecular interactions that occur during assembly is the first step toward this end.

Table 2: Thermodynamic Parameters for the High-Affinity Scaffolding Protein Binding Sites at Various Temperatures[a]

	10 °C	20 °C	30 °C	37 °C
stoichiometry[b]	39 (3); 40 (3)	58 (8); 56 (2)	87 (38); 61 (4)	80 (4); 82 (3)
K_d' (nM)	30 (38); 57 (56)	490 (510); 80 (45)	480 (6900); 3.5 (2.8)	22 (7); 16 (6)
$\Delta G^{\circ\prime}$ (kcal mol^{-1})	−9.8 (0.7); −9.4 (0.6)	−8.5 (0.6); −9.5 (0.3)	−8.8 (8.6); −12 (0.5)	−11 (0.8); −11 (0.2)
$\Delta H'$ (kcal mol^{-1})	−4.5 (0.7); −3.5 (0.7)	−13 (1) −6.2 (0.5)	−19 (3); −12 (0.4)	−23 (0.5); −18 (0.6)
$\Delta S^{\circ\prime}$ (cal mol^{-1} K^{-1})	+18 (3); +21 (3)	−11 (4); −11 (2)	−33 (30); −1.3 (2.1)	−39 (3); −21 (2)

[a] For each parameter, the value obtained by using an exponentially smoothed blank correction (see text) is listed first, followed by the value obtained by instead correcting with a linear regression of the final 5−10 points of the blank titration.[3] Nonlinear least-squares fits of the data to a model incorporating two sets of binding sites are shown in Figure 4A−D. [b] Number of scaffolding protein monomers bound per procapsid, assuming 420 coat protein subunits per procapsid.

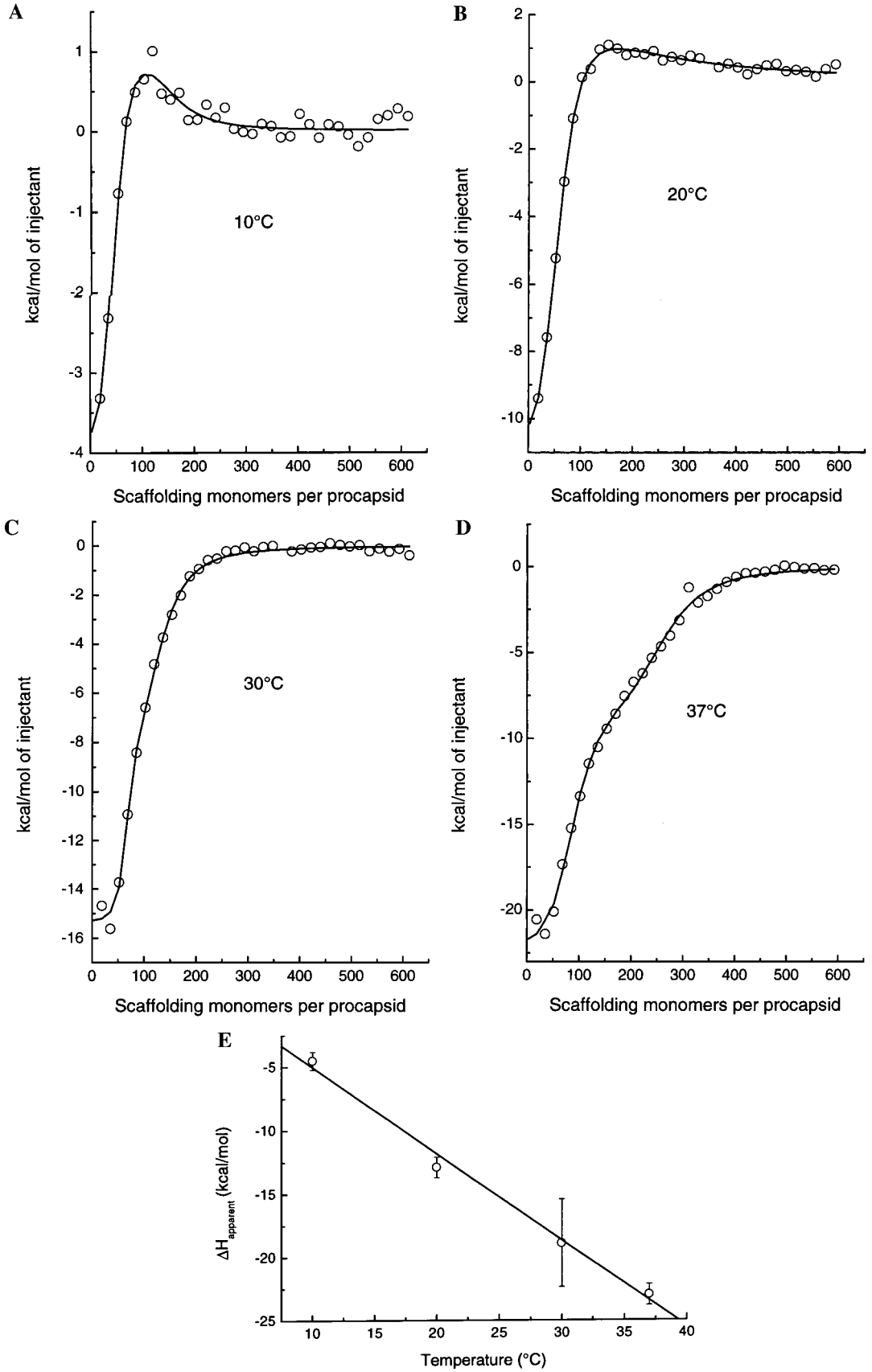

FIGURE 4: Negative changes in heat capacity accompany scaffolding protein binding to the high-affinity binding sites. (A−D) ITC data for experiments carried out in HEPES buffer at 10, 20, 30, and 37 °C, respectively. Note differences in the scales of the *y*-axes. (E) Plots of $\Delta H_{apparent}$ vs temperature. The slope gives the apparent ΔC_p.

The assembly pathway of the bacteriophage P22 is well understood at the molecular level (*16*), and has many similarities to the pathways used by pathogenic herpes- and adenoviruses. Many of the critical proteins involved in the assembly of P22 have been purified, and assembly can be analyzed in detail in vitro. P22 thus provides an excellent

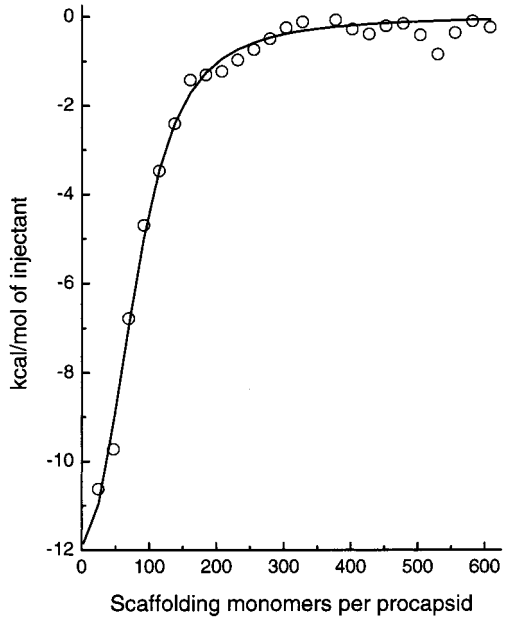

FIGURE 5: Scaffolding protein dimers bind to only one set of binding sites. Binding of the R74C/L177I covalent dimeric scaffolding protein mutant to procapsid shells was analyzed by ITC at 20 °C in HEPES buffer. Data were fit to a model incorporating a single set of binding sites. The data could not be fit to a model incorporating two sets of sites.

model system for studying the processes of viral assembly.

In the absence of the scaffolding protein, the P22 coat protein polymerizes only at high concentrations, and the resulting structures display aberrant morphology (*38*). Thus, the scaffolding protein serves to activate and control the assembly of the coat protein subunits. Biophysical studies have demonstrated that the scaffolding protein has a highly flexible, extended α-helical structure (*17*). A well-ordered C-terminal helix−loop−helix motif is responsible for binding to the coat protein (*26, 37*). Analytical ultracentrifugation has demonstrated that scaffolding protein monomers are in equilibrium with dimers and tetramers, and disulfide-cross-linked covalent dimers have been shown to be active in assembly (*18*).

The points of contact of the scaffolding and coat proteins within the procapsid lattice have been determined by electron cryomicroscopy. Based on these observations, a model for how scaffolding protein can direct assembly into the appropriate $T = 7$ structure has been proposed (*15*). According to this model, the key role played by the scaffolding protein is to direct and stabilize the formation of proper coat−coat interactions at certain critical positions in the procapsid.

Previous studies have suggested that there are two classes of scaffolding binding sites within the procapsid, and that only one class is absolutely required for assembly (*21, 30*). These studies were performed using kinetic analysis of assembly from coat protein monomers or of scaffolding reentry into procapsid shells, or by limiting the amount of scaffolding protein available during in vitro assembly and analyzing the composition of the resulting procapsids. In the present study, further kinetic experiments examined the behavior of a covalently cross-linked dimeric mutant scaffolding protein. The thermodynamic parameters for binding of scaffolding protein to procapsid shells were also measured by titration calorimetry. The use of procapsid shells allowed for the direct examination of scaffolding/coat binding interactions without the complicating factor of the formation of coat−coat interactions during procapsid assembly.

The kinetic experiments depicted in Figures 1 and 2 strongly suggest that the scaffolding protein binds to at least two distinct sets of binding sites, and that scaffolding protein dimers can bind to only one set. ITC experiments supported these conclusions (Figures 3−5; Tables 1 and 2). At 20 °C, approximately 60 scaffolding protein subunits bound to a high-affinity set of sites in each procapsid (Table 1). A lower-affinity set of binding sites was clearly detectable, although the stoichiometry and other thermodynamic parameters for binding to these sites could not be accurately determined. A covalently cross-linked dimeric scaffolding protein appeared to bind to only the high-affinity sites, with a stoichiometry of about 35 dimers per procapsid (Figure 5). Because these dimers can assemble procapsids (*18*), and they appear to bind only to the high-affinity sites, it is likely that this population of binding sites provides the critical binding interactions for the direction of form determination during procapsid assembly.

Binding to the high-affinity sites was accompanied by a large negative apparent ΔC_p (Figure 4; Tables 1 and 2). This term primarily reflects changes in the extent of hydration of the surfaces that become buried upon binding (*34−36*). Based on protein folding studies, empirical methods have been developed for estimating ΔC_p based on the total amounts of polar and apolar solvent-accessible surface area that become buried as the complex forms (*39, 40*). However, in some cases these predictions do not accurately predict the ΔC_p for protein−ligand binding processes. When this happens, the experimentally determined values are usually more negative than the predictions. This is most often observed in cases where water molecules become sequestered within the binding interface (*41−45*).

The complete structure of the scaffolding/coat protein binding interface is not known. However, the magnitude of the apparent ΔC_p value reported here is more negative than would be expected based on binding of the highly charged coat protein binding domain of the scaffolding protein to the complementary site on the coat protein [which is likely to be negatively charged (*28, 34, 46*)]. The complementary ionic surfaces in the scaffolding and coat proteins would be extensively hydrated in solution. While some of these water molecules would be displaced as the complex forms, any that remain would become more conformationally restricted. Ladbury et al. (*47*) have suggested that restriction of the degrees of freedom of water molecules within highly hydrated specific interfaces could make a substantial negative contribution to the ΔC_p for formation of the complex. A physical explanation for this phenomenon has been proposed (*48−50*).

An alternative explanation involves conformational change upon binding. In the binding of a dimeric transcription factor to DNA, Künne et al. (*51*) observed a large negative ΔC_p that was accompanied by the formation of additional helical structure in the protein. Raman spectroscopy has revealed that binding of the scaffolding protein to the procapsid causes an increase in the amount of α-helical structure in the scaffolding protein (*17*). This suggests that coupled conformational changes in the scaffolding and/or the coat proteins may accompany binding. These conformational changes

might also make negative contributions to the ΔC_p of scaffolding−coat binding.

From ITC experiments conducted in three buffers and at four temperatures (Figures 3 and 4; Tables 1 and 2), it is clear that at least two populations of binding sites, with quite different thermodynamic parameters, exist within the procapsid. Precise quantification of the thermodynamic parameters was challenging because of the rather large effects of the dissociation of scaffolding protein oligomers upon the overall heat signals (Figure 3A). Additional error can be introduced when fitting to a model that incorporates two distinct sets of binding sites, especially when the two transitions are not widely separated. We addressed this by analyzing the data in two ways: either by subtracting the heat effect of oligomer dissociation or by a simpler linear correction (see Materials and Methods). The results obtained from these two approaches were quantitatively very similar for the apparent stoichiometry value, and qualitatively similar for apparent $\Delta G°$, ΔH, and $\Delta S°$ (Table 1).

Thuman-Commike et al. (*15*) have proposed that the minimal contacts required for procapsid assembly involve the binding of 30 scaffolding protein dimers. We have found a stoichiometry of approximately 60 scaffolding monomers per procapsid for the high-affinity binding sites, supporting this model. Furthermore, the value determined by ITC is in general agreement with all previous attempts to determine this stoichiometry, both in binding to preformed procapsid shells (*24*, *30*) and in procapsid assembly from coat protein monomers (*21*, *24*). Further support comes from our finding that a covalent dimeric scaffolding protein appears to bind to only the high-affinity sites (Figure 5), and with approximately the stoichiometry predicted by Thuman-Commike (*15*).

Electrostatic interactions have been shown to play a major role in scaffolding/coat binding (*28*). We observed that 1 M NaCl causes a profound decrease in the magnitude of the exothermic heat signal of binding to the high-affinity sites (data not shown), suggesting that interactions involving charged residues are crucial to binding. In the case of the high-affinity sites, these interactions are dominated by a favorable enthalpy term. As discussed above, the large negative values for $\Delta C_p'$ are not what would normally be expected when binding is dominated by interactions between polar groups. These data are consistent, however, either with the formation of a binding interface that contains "bridging" hydrogen bonds formed by sequestered water molecules, or with conformational changes occurring upon binding.

In conclusion, light scattering and calorimetric experiments have demonstrated that the P22 scaffolding protein binds to at least two distinct sets of sites within the procapsid. Binding to the higher-affinity sites was driven primarily by a favorable enthalpy term between 10 and 37 °C. Data for the lower-affinity sites were more difficult to interpret due to low signal-to-noise ratios. However, binding to these sites changed from being entirely entropy-driven at 10 °C to having a favorable enthalpy term at 37 °C. The large negative value for $\Delta C_p'$ at the high-affinity sites suggests that the binding interactions include hydrogen bonds via "bridging" water molecules. Disulfide-cross-linked scaffolding protein dimers bound only to the high-affinity sites. As suggested in previous work (*28*), electrostatic interactions were found to play a major role in binding. The stoichiometry for the high-affinity sites was between 40 and 87 monomeric scaffolding subunits per procapsid, lending support to a model for procapsid assembly (*15*) in which 30 scaffolding dimers provide the critical interactions required for the direction of procapsid assembly.

ACKNOWLEDGMENT

We thank Kenneth W. French for excellent technical assistance, Prof. Sherwood Casjens (University of Utah) for the gift of the plasmid containing the coat, portal, and scaffolding protein genes, and Dr. Seng-Jao Soong (Biostatistics Unit, Comprehensive Cancer Center, University of Alabama at Birmingham) for advice on curve fitting.

REFERENCES

1. Hendrix, R. (1985) in *Virus Structure and Assembly* (Casjens, S., Ed.) pp 169−204, Jones and Bartlett, Boston.
2. Casjens, S., and Hendrix, R. (1988) in *The Bacteriophages* (Calendar, R., Ed.) pp 15−91, Plenum Press, New York.
3. Rixon, F. J. (1993) *Semin. Virol. 4*, 135−144.
4. Donaghy, G., and Jupp, R. (1995) *J. Virol. 69*, 1265−1270.
5. Hong, Z., Beaudet-Miller, M., Durkin, J., Zhang, R., and Kwong, A. D. (1996) *J. Virol. 70*, 533−540.
6. Newcomb, W. W., Homa, F. L., Thomsen, D. R., Booy, F. P., Trus, B. L., Steven, A. C., Spencer, J. V., and Brown, J. C. (1996) *J. Mol. Biol. 263*, 432−446.
7. Trus, B. L., Booy, F. P., Newcomb, W. W., Brown, J. C., Homa, F. L., Thomsen, D. R., and Steven, A. C. (1996) *J. Mol. Biol. 263*, 447−462.
8. Wood, L., Baxter, M., Plafker, S., and Gibson, W. (1997) *J. Virol. 71*, 179−190.
9. D'Halluin, J. C., Martin, G. R., Torpier, G., and Boulanger, P. A. (1978) *J. Virol. 26*, 357−363.
10. Prevelige, P. E., Jr. (1998) *Trends Biotechnol. 16*, 61−65.
11. Casjens, S. (1979) *J. Mol. Biol. 131*, 1−14.
12. Prasad, B. V. V., Prevelige, P. E., Marietta, E., Chen, R. O., Thomas, D., King, J., and Chiu, W. (1993) *J. Mol. Biol. 231*, 65−74.
13. Thuman-Commike, P. A., Greene, B., Jakana, J., Prasad, B. V., King, J., Prevelige, P. E., Jr., and Chiu, W. (1996) *J. Mol. Biol. 260*, 85−98.
14. Caspar, D. L. D., and Klug, A. (1962) *Cold Spring Harbor Symp. Quant.i Biol. 27*, 1−24.
15. Thuman-Commike, P. A., Greene, B., Malinski, J. A., Burbea, M., McGough, A., Chiu, W., and Prevelige, P. E., Jr. (1999) *Biophys. J. 76*, 3267−3277.
16. Prevelige, P. E., Jr., and King, J. (1993) *Prog. Med. Virol. 40*, 206−221.
17. Tuma, R., Prevelige, P. E., Jr., and Thomas, G. J., Jr. (1996) *Biochemistry 35*, 4619−4627.
18. Parker, M. H., Stafford, W. F., III, and Prevelige, P. E., Jr. (1997) *J. Mol. Biol. 268*, 655−665.
19. Berger, B., Shor, P. W., Tucker-Kellogg, L., and King, J. (1994) *Proc. Natl. Acad. Sci. U.S.A. 91*, 7732−7736.
20. Thuman-Commike, P. A., Greene, B., Malinski, J. A., King, J., and Chiu, W. (1998) *Biophys. J. 74*, 559−568.
21. Prevelige, P. E., Jr., Thomas, D., and King, J. (1988) *J. Mol. Biol. 202*, 743−757.
22. Casjens, S., and King, J. (1974) *J. Supramol. Struct. 2*, 202−224.
23. Eppler, K., Wyckoff, E., Goates, J., Parr, R., and Casjens, S. (1991) *Virology 183*, 519−538.
24. Parker, M. H., Casjens, S., and Prevelige, P. E., Jr. (1998) *J. Mol. Biol. 281*, 69−79.
25. Earnshaw, W. C., and Casjens, S. R. (1980) *Cell 21*, 319−331.
26. Parker, M. H., Jablonsky, M., Casjens, S., Sampson, L., Krishna, N. R., and Prevelige, P. E., Jr. (1997) *Protein Sci. 6*, 1583−1586.

27. Tuma, R., Parker, M. H., Weigele, P., Sampson, L., Sun, Y., Krishna, N. R., Casjens, S., Thomas, G. J., Jr., and Prevelige, P. E., Jr. (1998) *J. Mol. Biol. 281*, 81−94.
28. Parker, M. H., and Prevelige, P. E., Jr. (1998) *Virology 250*, 337−349.
29. Wiseman, T., Williston, S., Brandts, J. F., and Lin, L. N. (1989) *Anal. Biochem. 179*, 131−137.
30. Greene, B., and King, J. (1994) *Virology 205*, 188−197.
31. Teschke, C. M., King, J., and Prevelige, P. E., Jr. (1993) *Biochemistry 32*, 10658−10665.
32. Christensen, J. J., Hansen, L. D., and Izatt, R. M. (1976) *Handbook of proton ionization heats*, John Wiley & Sons, New York.
33. Fukada, H., and Takahashi, K. (1998) *Proteins: Struct., Funct., Genet. 33*, 159−166.
34. Sturtevant, J. M. (1977) *Proc. Natl. Acad. Sci. U.S.A. 74*, 2236−2240.
35. Gomez, J., Hilser, V. J., Xie, D., and Freire, E. (1995) *Proteins: Struct., Funct., Genet. 22*, 404−412.
36. Baldwin, R. L. (1986) *Proc. Natl. Acad. Sci. U.S.A. 83*, 8069−8072.
37. Sun, Y., Parker, M. H., Weigele, P., Casjens, S., Prevelige, P. E., Jr., and Krishna, N. R. (2000) *J. Mol. Biol. 297*, 1195−1202.
38. Earnshaw, W., and King, J. (1978) *J. Mol. Biol. 126*, 721−747.
39. Spolar, R. S., Livingstone, J. R., and Record, M. T., Jr. (1992) *Biochemistry 31*, 3947−3955.
40. Murphy, K. P., and Freire, E. (1992) *Adv. Protein Chem. 43*, 313−361.
41. Bhat, T. N., Bentley, G. A., Boulot, G., Greene, M. I., Tello, D., Dall'Acqua, W., Souchon, H., Schwarz, F. P., Mariuzza, R. A., and Poljak, R. J. (1994) *Proc. Natl. Acad. Sci. U.S.A. 91*, 1089−1093.
42. Ferrari, M. E., and Lohman, T. M. (1994) *Biochemistry 33*, 12896−12910.
43. Guinto, E. R., and Di Cera, E. (1996) *Biochemistry 35*, 8800−8804.
44. Pearce, K. H., Jr., Ultsch, M. H., Kelley, R. F., de Vos, A. M., and Wells, J. A. (1996) *Biochemistry 35*, 10300−10307.
45. Holdgate, G. A., Tunnicliffe, A., Ward, W. H., Weston, S. A., Rosenbrock, G., Barth, P. T., Taylor, I. W., Pauptit, R. A., and Timms, D. (1997) *Biochemistry 36*, 9663−9673.
46. Gallagher, K., and Sharp, K. (1998) *Biophys. J. 75*, 769−776.
47. Ladbury, J. E., Wright, J. G., Sturtevant, J. M., and Sigler, P. B. (1994) *J. Mol. Biol. 238*, 669−681.
48. Madan, B., and Sharp, K. (1996) *J. Phys. Chem. 100*, 7713−7721.
49. Madan, B., and Sharp, K. (1997) *J. Phys. Chem. B 101*, 11237−11242.
50. Sharp, K. A., and Madan, B. (1997) *J. Phys. Chem. B 101*, 4343−4348.
51. Künne, A. G. E., Sieber, M., Meierhans, D., and Allemann, R. K. (1998) *Biochemistry 37*, 4217−4223.
52. Burrows, S. D., Doyle, M. L., Murphy, K. P., Franklin, S. G., White, J. R., Brooks, I., McNulty, D. E., Scott, M. O., Knutson, J. R., Porter, D., Young, P. R., and Hensley, P. (1994) *Biochemistry 33*, 12741−12745.
53. Graversen, J. H., Sigurskjold, B. W., Thogersen, H. C., and Etzerodt, M. (2000) *Biochemistry 39*, 7414−7419.
54. Casella, G., and Berger, R. L. (1990) *Statistical Inference*, Duxbury Press, Belmont, CA.
55. Lovatt, M., Cooper, A., and Camilleri, P. (1996) *Eur. Biophys. J. 24*, 354−357.

BI0026167